ROLE OF SELENOPROTEIN P IN BRAIN ZINC HOMEOSTASIS

A THESIS SUBMITTED TO THE GRADUATE DIVISION OF THE UNIVERSITY OF HAWAI'I AT MANOA IN PARTIAL FULFILLMENT OF THE REQUIREMENTS FOR THE DEGREE OF

MASTER OF SCIENCE

IN

MOLECULAR BIOSCIENCES AND BIOENGINEERING

DECEMBER 2013

By

Arlene Rose Condaya Parubrub

Thesis Committee:
Frederick P. Bellinger, Chairperson
Robert A. Nichols
Jun Panee

Keywords: Selenoprotein P, brain zinc, Alzheimer's disease, selenium

ACKNOWLEDGEMENTS

This Master of Science thesis would not have been possible without the guidance and support of several individuals who provided invaluable assistance in the preparation and completion of this research.

First and foremost, I would like to acknowledge and express my gratitude to graduate advisor, Dr. Frederick P. Bellinger, whose intellectual expertise, constant encouragement, and indispensable mentorship enabled me to fully develop a comprehensive understanding of this study as I overcame all the obstacles in the completion of my research. His insightful comments and suggestions truly enhanced the creation of my thesis.

It is an honor for me to thank committee members, Dr. Robert A. Nichols and Dr. Jun Panee, for dedicating their time and knowledge, offering constructive criticism and comments, and challenging me to think even more critically about the content of my research.

I am indebted to my colleagues who have continuously supported me, especially the people of the Bellinger Lab, who created an enjoyable and memorable graduate school experience. Ms. Rachel Rueli, our lab technician, was always ready and willing to provide assistance whenever needed and took great care of the mice that I used for various experiments. Ms. Stephanie Barayuga sacrificed countless hours to harvesting mice tissue with me. I also thank Dr. Jane Uyehara-Lock for the many conversations we shared and for her insights and advice not only on academics but also on my career goals.

I would also like to acknowledge Mrs. Ann Hashimoto and Dr. Suguru Kurokawa from the Berry lab for their generosity in providing mice from their colony to fulfill the required sample size for my research and especially the mouse serum needed to perform the metal column purification experiment.

Finally, I owe my deepest gratitude to my family, my parents, siblings, and husband, whose undying love and support carried me throughout the duration of my graduate school career.

ABSTRACT

Selenoprotein P (Sepp1) is a selenium-rich antioxidant protein involved in extracellular transport of selenium (Se). Sepp1 also has metal binding properties. Zinc (Zn^{2+}) is an essential micronutrient that is released from terminals in the brain that utilize the neurotransmitter, glutamate. Both Zn^{2+} and Se are necessary for proper brain function. However, intracellular Zn^{2+} accumulation can contribute to neurotoxicity, and extracellular Zn^{2+} can promote aggregation of amyloid-beta to form brain plaques during development of Alzheimer's disease (AD).

Through metal column purification, we confirmed Sepp1's ability to bind Zn^{2+} as well as other biometals including Co^{2+} and Ni^{2+}. We investigated the role of Sepp1 in Zn^{2+} regulation by examining Zn^{2+} levels in wildtype (WT) and Sepp1 knockout ($Sepp1^{-/-}$) mice. Zinc-N-(6-methoxy-8-quinolyl)-ptoluenesulphonamide (TSQ) staining revealed increased levels of intracellular Zn^{2+} in the $Sepp1^{-/-}$ hippocampus, the region of the brain that is crucial to memory formation, compared to the WT mice. Mass spectrometry analysis of freshly frozen brain samples demonstrated a marked increase in total brain Zn^{2+} levels in the $Sepp1^{-/-}$ mice. Additionally, levels of key Zn^{2+}-regulating proteins in the brain are affected by the absence of Sepp1, possibly in response to the elevated Zn^{2+} content. However, live Zn^{2+} imaging of hippocampal slices with a selective extracellular fluorescent Zn^{2+} indicator (Fluozin-3) showed that $Sepp1^{-/-}$ mice have impaired Zn^{2+} release in response KCl-induced neuron depolarization, which may result in memory impairments.

Taken together, our findings reveal that Sepp1 plays a crucial role in the maintenance of Zn^{2+} homeostasis in the hippocampus and for proper brain function. The identification of a naturally occurring Zn^{2+}-chelator regulated by dietary selenium may significantly contribute to the treatment and prevention of AD.

TABLE OF CONTENTS

LIST OF TABLES

LIST OF FIGURES

CHAPTER 1.

CHAPTER III.

LIST OF ABBREVIATIONS

Aβ	amyloid-beta
AD	Alzheimer's Disease
APP	amyloid precursor protein
ASK1	apoptosis signaling regulating kinase 1
BACE	β-secretase
C99	C-terminal stub
CAA	cerebral amyloid angiopathy
CQ	cliquinol; 5-chloro-7-iodo-8-hydroxyquinoline
CSF	cerebrospinal fluid
DIO	iodothyronine deiodinase
EFsec	sec-tRNA specific elongation factor
Gpx	glutathione peroxidase
KEGG	Kyoto Encyclopedia of Genes and Genomes
KCC2	potassium/chloride co-transporter
LOAD	late onset AD
LTP	long-term potentiation
MPAC	metal-protein attenuation compounds
N2A	Neuro-2a neuroblastoma cells
NFT	neurofibrillary tangles
NT	neurotransmitter
PP2A	protein phosphatase 2A
RDA	recommended daily allowance
ROS	reactive oxygen species
SBP2	SECIS-binding protein 2
Se	selenium
Sec	selenocysteine
SECIS	selenocysteine insertion sequence
Sec-tRNA	selenocysteine-specific tRNA
Sepp1	selenoprotein P

SPS2	selenophosphate synthase 2
SVZ	synaptic vesicle zinc
TrxR	thioredoxin reductase
U	Sec
VGCC	voltage-gated calcium channels
Zn^{2+}	zinc
ZnT	zinc transporter
ZIP	Zrt-Irt-like protein

CHAPTER I

INTRODUCTION

Alzheimer's Disease

Background

Alzheimer's disease (AD) is the most common neurodegenerative disorder and the major cause of dementia among the elderly [38]. Consequently, AD is one of the most critical global health issues. Alzheimer's Disease International states that AD affects greater than 35.6 million people worldwide with a few treatments that are only mildly effective to slow its progression. An estimated 5.3 million Americans have been diagnosed with AD, including 1 out of every 9 individuals over the age of 65. Most AD cases begin after 65 years old; the possibility of having AD is positively correlated with age. As of 2013, the cost of care for patients with AD is approximately $203 billion and is expected to rise to $1.2 trillion by 2050 [74].

This disease is characterized by amyloid plaques originating from amyloid-beta (Aβ) peptide aggregation, neurofibrillary tangles (NFTs) from hyperphosphorylated, aggregated tau, and extensive neuronal loss. Chronic increased levels of Aβ (predominantly Aβ42) in the brain and/or impaired clearance of Aβ from the brain leads to AD pathology and ultimately dementia [38, 40].

Clinical features of AD and pathology

AD causes dementia, the loss and decline in memory and other cognitive abilities that interfere with normal activities and relationships. It accounts for 60-70% of dementia cases, while other cases result from vascular dementia, Lewy body dementia, and frontotemporal dementia. The general time course of AD dementia is over an average span of 7-10 years, which ultimately culminates in patient death.

The amyloid plaques are comprised of Aβ peptides, generally 38-43 amino acids in length and are cleaved from the amyloid precursor protein (APP). Highly expressed in CNS neurons, the APP is an integral cell membrane protein with a single membrane-spanning region [44]. Alternative mRNA splicing results in several isoforms, with the most common isoforms

having lengths of 695, 751, and 770 amino acid residues. Specific proteolytic enzymes, β-secretase (BACE), γ-secretase, and α-secretase, can cleave APP on three different sites, resulting in smaller polypeptides. β-secretase cleaves the APP ectodomain and generates a soluble APP fragment and a membrane anchored C-terminal stub (C99), which is subsequently cleaved by γ-secretase to produce Aβ. An alternate processing pathway from α-secretase cleavage along with γ-secretase creates a soluble, non-amyloidogenic product [42]. γ-secretase can cleave APP at varying amino acid sites within the membrane: 38, 39, 40, 42, and 43 at the C-terminal end of Aβ.

Aβ is in abundant levels within the CSF at 10-20ng/mL and is found in lower levels in the plasma [35]. The two commonly produced Aβ isoforms are Aβ40 and Aβ42. The most abundant isoform in normal brain is Aβ40, which is localized in the CSF. Due to its hydrophobicity and likelihood to aggregate, the Aβ42 can initiate Aβ aggregation. Other isoforms such as Aβ 1-28 is derived from the APP region outside the membrane. Aβ 29-43 is derived from the APP region within the membrane-spanning region [40].

Aβ plaques aggregation initiates within the cerebral cortex and hippocampus of AD patients and progressively spreads throughout the brain [15]. The plaques are surrounded by swollen, degenerating neurites, generally from axons and dendrites. Despite accumulation of plaques over the course of AD, however, there is abundant evidence to show that it is soluble oligomers of Aβ which trigger neurotoxicity [38, 40].

Several studies have shown that tau plays a key role in AD pathology. Tau is produced in all neurons and in glia. Its function is to bind to tubulin and stabilize axonal microtubules. When tau is hyperphosphorylated, it dissociates from the microtubules and self-aggregates to form NFTs in neuronal cell bodies, which contributes to neuronal dysfunction. NFTs are also, however, found in other brain disorders such as frontotemporal dementias and progressive supranuclear palsy [4] in the absence of Aβ accumulation.

Neuropil threads, anomalous structures mainly located in distal dendrites and co-localized with NFTs and senile plaques, are also a product of hyperphosphorylated, aggregated tau and a morphological hallmark of AD. Recent findings have demonstrated a link between elevation of oligomeric Aβ and tau hyperphosphorylation-based mislocalization [37].

Other pathological hallmarks of AD include synaptic degeneration [21], specific neuronal cell death, decrease in expression of certain neurotransmitter (NT) markers such as choline acetyltransferase and dopamine activity [61] and loss or impaired function of basal forebrain cholinergic neurons. Neurons that are vulnerable to AD are located in layer II of the entorhinal cortex, hippocampal pyramidal layers, and areas of the temporal, parietal, and frontal neocortex [40].

Research progress

AD is the only cause of death among the top 10 in America that has no current means of prevention, cure, or treatments to slow its progression (www.alz.org). Advances in multiple fields such as neuroscience, biochemistry, and genetics have expanded our knowledge in the myriad of complex pathways, processes, and molecules involved in AD pathogenesis.

There is evidence showing that inhibiting or reversing Aβ or tau aggregation may delay the onset or slow progression of AD. Possible treatments include decreasing insoluble Aβ production, neutralizing Aβ toxicity, and enhancing Aβ clearance [40]. Drugs that can potentially delay onset of AD are difficult to test in clinical trials due to the challenge in finding a large patient population who is at high risk of becoming cognitively impaired within a 3-4 year window for clinical trials.

Currently only two classes of drugs are approved for treatment of AD. These include acetylcholinesterase inhibitors and the NMDA antagonist memantine. These drugs will give short-term improvements and delay progression in some patients, but become less effective with continued use. The cholinergic neurons are normally involved in attention and memory and have been the basis for "cholinergic therapy" in AD. The "cholinergic hypothesis", developed 20 years ago, stipulates that a loss of cholinergic function in the CNS can greatly attribute to the overall cognitive decline associated with both aging and AD [5]. By inhibiting CNS cholinesterase, the enzyme that degrades the neurotransmitter acetylcholine, AD patients can experience modest symptomatic relief [29]. Other modest symptomatic treatments include memantine, generally restricted to patients of moderate to severe AD, which modulates the NMDA subtype of glutamate receptors [3].

Studies are in progress to identify AD biomarkers that can detect early onset AD-pathology, such as Aβ accumulation and neurodegeneration in individuals who are

cognitively normal. Some experimental positron emission molecular probes can effectively detect the presence or absence and quantify the amount of amyloid in living individuals [22]. In addition, the levels of Aβ42 and tau in cerebrospinal fluid (CSF) can determine the presence of amyloid accumulation and neurodegeneration [59].

Selenoprotein background

Known functions of several selenoproteins

Selenoproteins contain selenium (Se) in the form of the 21st amino acid, selenocysteine (Sec). Se is an essential micronutrient for mammalian life and plays a major role in multiple physiological processes. It is metabolized through dietary selenium intake. Common dietary sources of Se include vegetables, fish, red meat, eggs, and poultry. The Se content of the soil can also affect one's Se intake.

Selenoproteins include three families of well-studied eukaryotic enzymes. Thioredoxin reductases (TrxR), specifically Txnd1, TrxR2, and TrxR3, are found primarily in mammals and are crucial in reducing peroxide [8]. They modulate apoptosis to control cell division, longevity, and cell death by inhibiting apoptosis signaling regulating kinase 1 (ASK1) [62]. The glutathione peroxidases (Gpx), notably GPx1, GPx2, GPx3, GPx4, and GPx6, utilize the antioxidant glutathione to reduce peroxides and other reactive oxygen species (ROS) that could damage cells and tissues [39, 52]. The iodothyronine deiodinases (DIO) participate in the synthesis and metabolism of thyroid hormones [6].

Other selenoproteins are involved in a variety of biological functions ranging from reducing ER stress, gene regulation, and producing phospholipids [56, 77].

Structure and synthesis

Dietary selenite is reduced to selenide via glutathione-glutaredoxin and thioredoxin pathways. Selenide is converted to monoselenophosphate by the selenophosphate synthase 2 (SPS2) enzyme. Selenocysteine synthetase adds monoselenophosphate to a phosphoserine residue conjugated to selenocysteine-specific tRNA (sec-tRNA) to generate Sec for selenoprotein production. The sec-tRNA is unique because it is encoded by the UGA codon, which is a stop codon in non-selenoprotein genes [65].

In order to properly translate the selenocysteine codon, the selenocysteine insertion

sequence (SECIS), a distinct stem-loop 2° structure on the 3' end of the untranslated region in all selenoprotein mRNA promotes proper read-through and insertion of Sec at the UGA codon. The unique stem-loop 2º structure binds for the SECIS-binding protein 2 (SBP2), which results in the recruitment of sec-tRNA specific elongation factor (EFsec) [66]. Assembly of the transcription factors on selenoprotein mRNA prepares for the proper coding of UGA as Sec [8, 9].

Selenium and AD

Recent studies have demonstrated that Se produced in different proteins can alleviate AD pathology in cell culture and in animal studies. Seleno-L-methioneine safeguards against oxidative stress and toxicity from Aβ peptides [51, 78]. Sodium selenate can decrease NFT formation by acting as an agonist for protein phosphatase 2A (PP2A) thus reducing tau phosphorylation [24]. Additionally, sodium selenite can inhibit Aβ production by down regulating γ-secretase activity, which lessens AD pathology and cognitive dysfunction in streptozotocin-induced rodent model of AD [74].

Selenoprotein P

Known functions

Selenoprotein P (Sepp1) is a selenium-rich secreted extracellular protein that is crucial for Se homeostasis and transport from the liver and peripheral tissues. Sepp1 is primarily secreted in the liver, but is also abundant in serum and widely throughout the body based on findings that Sepp1 mRNA is present in most tissues. $Sepp1^{-/-}$ mice have decreased Se levels in the brain, suggesting its role in Se transport [11].

Findings also suggest that Sepp1 has a function in oxidant defense [13, 31]. Cell culture studies have shown that Sepp1 participates in protecting Gpx against ROS in astrocytes cultured in Se-free medium [68]. Sepp1 up regulation is age-dependent and crucial for selenoenzyme expression (e.g. GPx4) [31, 52].

Sepp1 may be necessary for proper synaptic transmission and synaptic plasticity. Neuronal expression of Sepp1 in hippocampal cells is necessary for long-term potentiation (LTP), a cellular model for learning and memory. Sepp1$^{-/-}$ mice exhibit deficient synaptic function of the hippocampus, a disruption in spatial learning, and a severe deficit in LTP even when fed a high Se diet [60].

Structure, metal binding region

Sepp1 is unique in that it has 10 Sec residues, while most selenoproteins only have one. Figure 1 shows Sepp1's two functional, glycosylated domains: 1) a Se-rich C-terminal domain with 9 Sec residues, 2) an N-terminal domain with 1 Sec (U) in U-x-x-C redox motif, 2 histidine-rich metal binding sites (located at residue 204-217 and residue 244-250) and 1 heparin binding site [11]. Sepp1 has an N-terminal signal peptide for extracellular secretion, which is cleaved in the Golgi. The redox and His-rich motif reportedly have strong affinity to Cu^{2+} and Zn^{2+} ions [28].

According to the Kyoto Encyclopedia of Genes and Genomes (KEGG) database, the human Sepp1 protein structure has a zinc-binding domain overlapping one of the His-rich regions, which has homology to the ZIP zinc transporter domain. Additionally, within this sequence is a zincin Zn^{2+}-binding motif, generally found in the metzincin family of metalloproteases [36]. Table 1 portrays how the Sepp1 sequence aligns with other zincin-containing Zn^{2+} proteins, proteases, and members of the ZIP motif, suggesting a role in chelation and/or transport of brain Zn^{2+}.

Sepp1 and AD

The brain demands an abundance of energy and oxygen resulting in a high amount of oxidizable metals. Therefore, the brain is reliant on several selenoproteins for antioxidant function [7]. Recent findings indicate Sepp1's association with various hallmarks of AD pathology. Sepp1 co-localizes with Aβ plaques and NFTs in postmortem human cortex [8]. Sepp1 protein levels are increased in AD brain while Sepp1 knockdown leads to neurotoxicity from Aβ. In cell culture studies, Sepp1 knockdown had increased Neuro-2A (N2A) neuroblastoma cell sensitivity to Aβ toxicity [72]. Further studies indicated that a region of Sepp1 containing the putative zinc-binding domain can assist in protecting N2A

cells from controlled Aβ42 fibrillar toxicity [28].

Sepp1 binds to two low-density lipoprotein receptors, ApoER2 and megalin. ApoER2 appears to be necessary for uptake of Sepp1 to the brain and testes, while megalin in kidney removes Sepp1 from urine. These receptors also bind ApoE, which influences the clearance of soluble Aβ and the potential for insoluble Aβ to aggregate via Aβ seeding and polymerization [47]. ApoE helps to maintain synaptogenesis and synaptic connection by transporting cholesterol-rich lipoproteins to neurons [16]. The ApoE4 allele of ApoE increases risk of late onset AD (LOAD) and cerebral amyloid angiopathy (CAA) [25, 40]. The ApoE genotype is strongly associated with Aβ phenotype, particularly Aβ deposition and CSF Aβ42 levels but not CSF tau levels [40]. Megalin clears Aβ from the brain through the choroid plexus, and polymorphisms of this protein may also increase risk of AD. ApoER and megalin$^{-/-}$ mice are deficient in brain Se, indicating that both proteins regulate Se homeostasis through Sepp1 binding. Megalin$^{-/-}$ animals may have a reduction in total Se rather than specifically brain Se, which may mean that megalin recovers Sepp1 and prevents urinary secretion of Se [12].

Zinc

Function in body

Zn^{2+} is an important multipurpose trace element with major biological roles. Zn^{2+} is a component of enzymes that regulate multiple processes including DNA synthesis, brain development, reproduction, membrane stability, and bone formation. The Zn^{2+} structural role is important for DNA-binding proteins such as transcription factors and other proteins containing "Zn^{2+} fingers" and is found in the active site of metalloenzymes [74]. Additionally, Zn^{2+} is an essential regulatory ion in homeostatic processes such as absorption, distribution, cellular uptake, and excretion [18]. It also participates in immunity, intermediary metabolism, DNA metabolism and repair, vision, and taste acuity, cognition and behavior [53].

Under normal physiological conditions, Zn^{2+} protects the cell from oxidative damage in a number of ways including maintaining adequate MT levels, stabilizing cell membrane structure, and functioning as an essential component of superoxide dismutase. Zn^{2+} deficiency increases oxidative damage in lipids, proteins, and DNA [53].

Function in the brain

Zn^{2+} is involved in various functions in the brain, including neurotransmission, axonal transport, and neuromodulation [18]. Twenty percent of total Zn^{2+} ions are stored in high levels (~1mM) within Zn^{2+} synaptic vesicles of a subset of specialized glutamatergic neurons termed "gluzinergic" neurons [75]. Gluzinergic neurons contribute to 50% of all glutamatergic synapses [32]. Synaptic vesicle Zn^{2+} (SVZ) is assumed to be in the free ionic or loosely bound state because they can be easily visualized via histochemistry with stains that require chelation of free Zn^{2+} [26]. SVZ is released in an activity-dependent manner from specific terminals in the brain that utilize the neurotransmitter glutamate [53]. Glutamate is the major excitatory neurotransmitter that mediates synaptic transmission and plasticity [76]. The hippocampal mossy fibre axons terminals are rich in SVZ, which are found throughout the hippocampus, cortex, and striatum.

Zn^{2+} modulates the overall excitability of the brain by affecting glutamate receptors and possibly GABA receptors with a potential role in synaptic plasticity [32]. For instance, Zn^{2+} may reduce postsynaptic LTP in the CA3 hippocampus in order to stimulate presynaptic LTP. Zn^{2+} can also inhibit NMDA-dependent LTP induction by binding to the high affinity domain on the N-terminal region of specific subunits of NMDA receptors [43]. Additionally, Zn^{2+} inhibits presynaptic release by binding to other receptors with lower affinity to either activate ATP-sensitive K^+ channels or block voltage-gated Ca^{2+} channels (VGCC) [71]. A newly discovered Zn^{2+} receptor, GPR39, is known to increase GABA receptor response by moderating intracellular chloride levels through the K^+/Cl^- co-transporter, KCC2 [20].

Zn^{2+}pathology

Adult humans have 2-3 g of Zn^{2+} and approximately 0.1% is replenished daily. The recommended daily allowance (RDA) is 11mg for adult men and 8mg for women (Office of Dietary Supplements, NIH). Zn^{2+} is found in all body tissues with 85% residing in muscle and bone, 11% in skin and liver, and 2-3% in all other tissues. Our bones contain a third of whole body Zn^{2+}, marking a significant source of endogenous Zn^{2+} when the dietary supply is low [47].

More than 25% of the world population is at risk of Zn^{2+} deficiency. Contributing factors include poverty, limited food availability, and food preferences. Consumption of nutritional

supplements can substantially increase Zn^{2+} intake. A major source of dietary Zn^{2+} comes from legumes and cereal. Red meat is the richest in Zn^{2+}, poultry and fish contain much less, while dairy products hold approximately 20% of Zn^{2+} [53].

Some physical signs of Zn^{2+} deficiency include poor growth and retarded development in children and adolescents, dermatitis or skin inflammation, and poor healing of cutaneous wounds. Effects to the nervous system include decreased nerve conduction, disorientation, and impaired neuropsychological performance [53].

Excess Zn^{2+}, generally from dietary intake, leads to heavy metal poisoning with symptoms such as nausea, abdominal cramping, vomiting, diarrhea, and decreased urine output [53]. It can also suppress Cu^{2+} and Fe^{2+} absorption resulting in anemia. Free Zn^{2+} ions are powerful Lewis acids that can be corrosive when it reacts with hydrochloric acid in the stomach, which generates zinc chloride and damages the stomach lining [10].

Regulation of Zn^{2+}

Intracellular Zn^{2+} is regulated by Zn^{2+} transporters (ZnT), the Zrt-Irt-like protein (ZIP) family, and metallothioneins (MT) (Figure 2). There are twelve ZIP genes in humans, three in mice. hZIP1 and hZIP2 are involved in zinc uptake across the plasma membrane [34].

There are four putative mammalian ZnTs [41, 54, 57, 58] that each has multiple membrane-spanning regions and a His-rich loop oriented towards the cytosolic side. ZnT1, 3, and 4 are all localized in the brain, each with slightly different interactions with Zn^{2+}. ZnT1 is a Zn^{2+} exporter located in the plasma membrane and is expressed ubiquitously [75].

ZnT3 is a synaptic Zn^{2+} transporter that is restricted to the brain and testis. It is the most commonly studied ZnT protein. In the brain, it is localized in the membrane of synaptic vesicles with increased expression and distribution in the CA4 hilar region of the dentate gyrus, stratum lucida of CA3, and the pyramidal cells of the CA1 and CA3 regions. ZnT3 is involved in Zn^{2+} packaging and loading into synaptic vesicles [32]. $ZnT3^{-/-}$ mice have no Zn^{2+} in the synaptic terminals suggesting that ZnT3 is responsible for loading Zn^{2+} into the synaptic vesicles [70].

ZnT3 may also be crucial in the uptake of vesicular Zn^{2+} needed for early binding proteins, such as various metalloenzymes and zinc finger transcription factors. Furthermore, ZnT3 expression in neocortical areas correlate with the distribution of gluzinergic neurons but not

with the distribution of SVZ cells, indicating the presence of different transporters involved in Zn^{2+} uptake into vesicles [68].

Metallothionein oversees the homeostasis of intracellular free Zn^{2+} levels. It also modulates the transfer of Zn^{2+} to cytoplasmic and nuclear proteins, such as transcription factors, that contain the Zn^{2+} finger domain. Due to their limited biological half-life, MTs do not provide long-term Zn^{2+} storage. The two most abundant isoforms in the brain are MT3 and MT4 [75]. MT3 is the primary Zn^{2+} storage protein in neurons. MT3 levels are low in AD brain extracts further suggesting that MT may protect neurons from oxidative stress and modulate neurotransmission [26, 67].

Zn^{2+} and AD

Although Zn^{2+} may be necessary for proper brain function, intracellular Zn^{2+} accumulation can contribute to neurotoxicity, while extracellular Zn^{2+} can promote aggregation of Aβ to form brain plaques during development of AD [2]. Due to the need for many proteins involved in Zn^{2+} homeostasis, there is an increased potential for variations in Zn^{2+} metabolism due to mutations. Acrodermatitis enteropathica, for instance, is a genetic disorder of Zn^{2+} absorption in humans linked to a mutation in Zn^{2+} transporter hZIP4 [53].

Zn^{2+} metabolism is altered in AD pathophysiology resulting in an abnormally enriched Zn^{2+} environment [30]. In postmortem AD brain, Zn^{2+} is found at significant levels in association with Aβ plaques. Aβ and synaptic Zn^{2+} are co-distributed, mainly at the excitatory synapses where there is increased synaptic Zn^{2+} release [48] (Figure 2). Excess synaptic Zn^{2+} in the synaptic cleft may be attracted to Zn^{2+}-binding sites on the Aβ peptide inducing Aβ oligomerization. Zn^{2+} taken up by the Aβ peptides is diverted away from essential postsynaptic receptors (e.g. NMDA) potentially contributing to cognitive decline [63].

In $ZnT3^{-/-}$ and APP-overexpressing mutant mouse brains, there is a decrease in plaque load and lower levels of insoluble Aβ. This suggests synaptic Zn^{2+}'s role in Aβ generation and aggregation [18]. By chelating extracellular Zn^{2+} and possibly other metals, Sepp1 may participate in Zn^{2+} and overall biometal homeostasis in the brain.

Current breakthroughs (chelating biometals)

Basic research studies and clinical trials have investigated the use of Zn^{2+} chelators and regulators, also known as metal-protein attenuation compounds (MPACs), for the prevention and treatment of neurodegenerative disorders by potentially sequestering Zn^{2+} from Aβ plaques and at the synaptic cleft [14]. Zn^{2+} chelating agents such as 5-chloro-7-iodo-8-hydroxyquinoline (clioquinol; CQ) and DP-109 can modulate brain Zn^{2+} levels and can inhibit amyloid plaque formation. CQ is a Zn^{2+} and Cu^{2+} chelator that showed promise in decreasing the size and volume of Aβ plaques in transgenic mice [19]. However, studies also report that systemic CQ promotes myelinopathies in the CNS of transgenic AD mice and their littermate controls [80], which may be a result of CQ's ability to also chelate Cu^{2+}.

PBT2, a second-generation 8-OH quinolone derivative of CQ may also aid in neuroprotection and delay cognitive impairment in an AD transgenic model [1] by potentially enhancing intracellular Zn^{2+} and Cu^{2+} uptake. PBT2 acts as a chelator that allows the clearance of these ions from the parenchymal Aβ plaques and synaptic space [27]. This CQ derivative in currently the subject of Phase II IMAGINE clinical trial for AD, and Phase II Reach2HD clinical trial for Huntington's Disease. Both trials will release their results in 2014 (www.pranabio.com).

Other known metal chelators (e.g. metallothionein) may prevent metal-induced Aβ42 non-fibrillar aggregation by removing metal ions from Aβ42. The characterization of a naturally occurring Zn^{2+} binding protein regulated by dietary selenium may be of potential use in the treatment and prevention of AD.

Interactions between Zn^{2+} and Sepp1

The high affinity of free Se to free Zn^{2+} has been utilized for various histological methods in neuroscience research as originally demonstrated by the Danscher method, which detects SVZ cells by precipitation of Zn^{2+} ions with sulphide or selenium salt (Figure 3) [69]. However, the biological relevance of this interaction has yet to be explored.

Zn^{2+} participates in stabilizing the structure of numerous DNA binding proteins by binding to cysteine and histidine rich side chains in a tetrahedral conformation [79]. It is predicted that the two His-rich regions of Sepp1 may allow binding of Zn^{2+} in a similar fashion.

Zn^{2+} significantly enhances Aβ42 toxicity towards N2A cells, demonstrating that metal

associated Aβ species have a neurotoxic feature. Furthermore, Sepp1 enhanced the survival rate of N2A cells treated with Zn^{2+}- Aβ42 and diminished neurotoxicity of Zn^{2+}- Aβ42 complex, suggesting that Sepp1 is able to detach Zn^{2+} from the protein complex, allowing the free Aβ42 to produce fibrils that are less toxic than its Zn^{2+}- induced aggregate. Current evidence supports a potential role for Sepp1 to chelate metal ions and interact with Aβ42, possibly via the His-rich domains [28].

With focus on the hippocampus, a brain structure involved in learning and memory, this study investigates the role of Sepp1 in brain Zn^{2+} regulation by comparing Zn^{2+} levels in wild type (WT) and $Sepp1^{-/-}$ mice. We aim to characterize the biological significance of Sepp1 in brain Zn^{2+} homeostasis by addressing key questions that will elucidate the mechanistic nature of Sepp1. How does Sepp1 affect Zn^{2+} levels and regulation in the brain? Do $Sepp1^{-/-}$ animals have changes in synaptic Zn^{2+} release that may affect synaptic physiology? Due to the presence of two metal-binding domains on Sepp1, we predict that Sepp1 can regulate brain Zn^{2+} homeostasis by removing or chelating excess Zn^{2+} in hippocampal neuron.

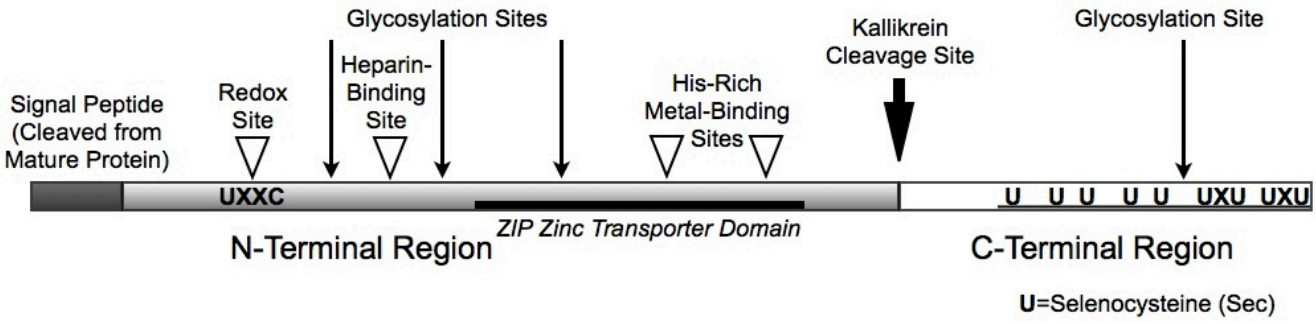

Figure 1. Schematic of Sepp1 structure. The N-terminal region has one Sec (U) in a redox domain, a heparin-binding site and a zinc transporter domain with two metal-binding sites. The C-terminal region has 9 Sec residues for Se transport.

Table 1. Alignment of human Sepp1 metal binding region with other proteins containing the zincin motif.

		Zincin Domain:	-**HE**XX**H**-
	Sepp1	206...217	H**HE**HH**H**NHGHQH
Zinc transporters	Zip4	500...600	C**HE**LP**H**ELGDFA
	Zip5	422...432	C**HE**LP**H**ELGDFA
	Zip9	92...102	V**HE**HE**H**SHDHTQ
	Zip10	616...625	I**HE**HD**H**GPELH
Metalloproteases	ADAM 9	347...357	A**HE**LG**H**NLGMNH
	ADAM 10	383...393	A**HE**VG**H**NFGSPH
	MMP1	217...227	A**HE**LG**H**SLGLSH
	MMP2	208...218	A**HE**IG**H**SLGLFH
	MMP9	401...410	A**HE**FG**H**ALGLDH
	Neprilysin	584...594	G**HE**IT**H**GFDDNG

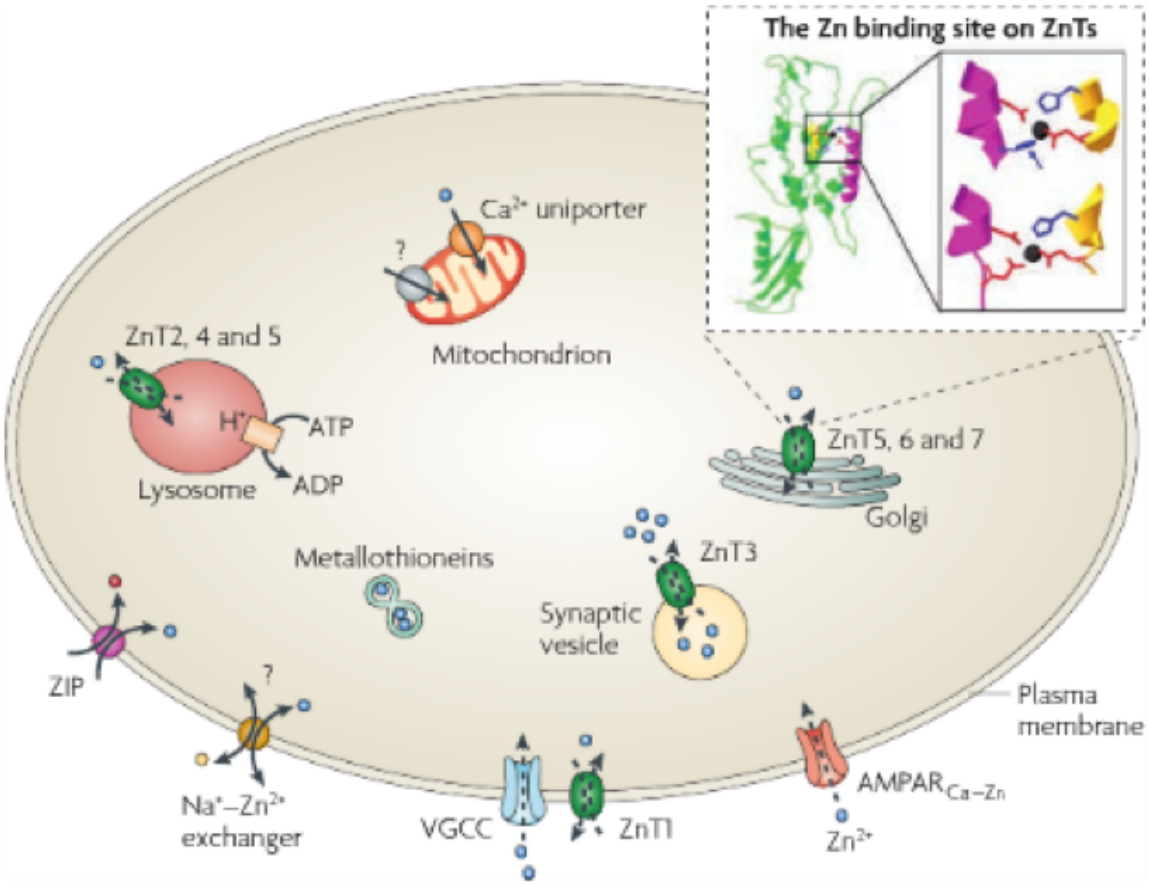

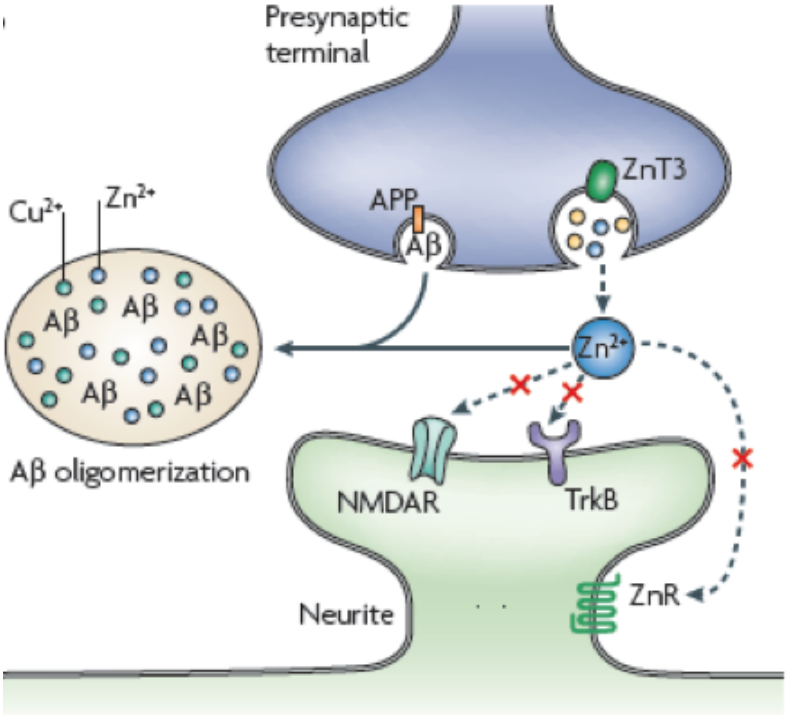

Figure 2. Regulation of Zn^{2+} and the implications of Zn^{2+} in AD pathology. Above: diagram of Zn^{2+} regulating proteins. Below: proposed mechanism of Zn^{2+}'s role in AD pathology. Reference: Sensi, S.L. et al. (2009) Zinc in the physiology and pathology of the CNS. *Nature reviews neuroscience*, **10**, 780-791.

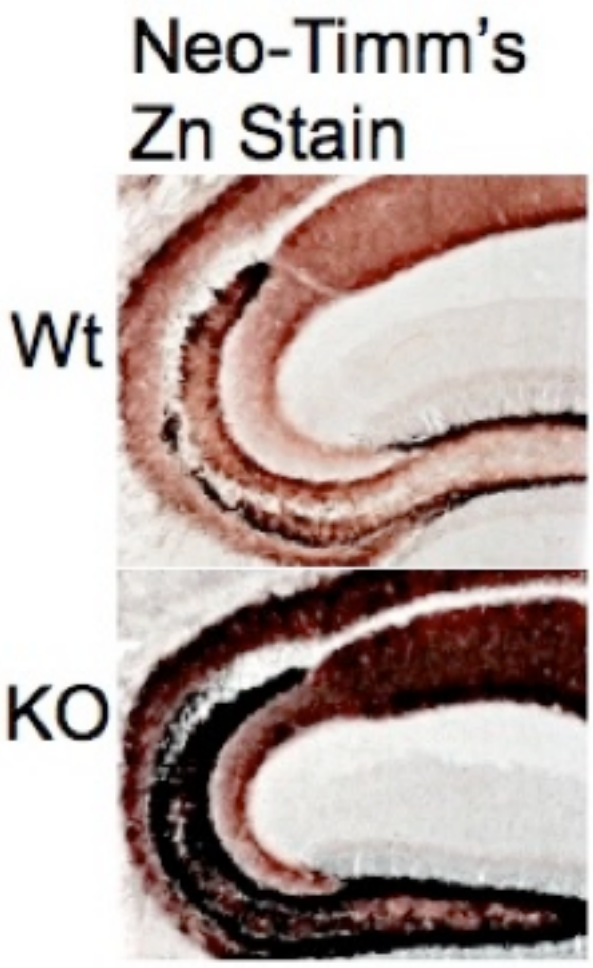

Figure 3. Neo-Timm's (Danscher) stain. Free Zn^{2+} in wildtype and $Sepp1^{-/-}$ hippocampal neurons from mice injected with sodium selenite is revealed as a reddish-brown to dark brown color relative to the amount of total Zn^{2+}.

CHAPTER II

MATERIALS AND METHODS

Animals

Mice were group housed on a 12 hour light cycle and provided food and water *ad libidum*. All animals in this study were maintained on diets containing adequate Se (~0.25 ppm) unless otherwise noted. All animal procedures were approved by the University of Hawaii Institutional Animal Care and Use Committee.

Generation of Sepp1$^{-/-}$ mice

Sepp1$^{-/-}$ mice were obtained from the laboratory of Dr. Raymond Burk at Vanderbilt University. The mutant mice were backcrossed to C57BL/6J for at least ten generations with C57BL/6J mice from Jackson Laboratories to ensure congenic strains. Breeding of the Sepp1$^{+/-}$ mice generated littermates of Sepp1$^{+/+}$ and Sepp1$^{-/-}$ pups, which were used in this study in addition to Sepp1$^{+/-}$ mice. Genomic DNA extracted from mouse tails was used for genotyping PCR using specific primers (forward-ACCTCAGCAATGTGGAGAAGCC, reverse-TGCCCTCTGAGTTTAGCATTG). Products were run on a 1.5% DNA agarose gel with a SYBR Safe DNA gel stain (Invitrogen) and genotypes were confirmed under UV light.

Tissue preparation

Three-month-old mice (24 Sepp1 KO animals and 24 littermate controls, both male and female) were euthanized with CO_2 gas followed by rapid decapitation. The brains were removed and frozen rapidly on dry ice and bisected into hemispheres (left hemispheres for ICP-OES, and right hemispheres for histology). Liver was also isolated from each animal as a control tissue for ICP-OES.

6-Methoxy-8-p-Toluenesulfonamido-Quinoline (TSQ) stain

TSQ is a common Zn^{2+} fluorophore that binds cellular Zn^{2+} in a 2:1 ligand-to-metal ratio that results in increased fluorescence emission at 490 nm in response to excitation at 360 nm [55]. 10 μm thick sagittal cryosections of frozen left brain hemisphere were mounted on positively charged microscope slides. The slides were immersed with 4.5μM TSQ (Enzo

Lifesciences, UltraPure) in 140mM sodium barbital and 140mM sodium acetate buffer (pH 10) for 90 seconds, as previously described [33] and washed in 0.1% NaCl. TSQ-stained sections were imaged using DAPI filter settings (200ms, monochrome with a 5x objective). The mean fluorescence intensity of the CA1 stratum oriens and stratum radiatum, CA3 mossy fibers, and hilar region were measured with ImageJ software (NIH). The background was measured in unstained areas within lateral ventricles and subtracted from mean TSQ signals.

Inductively Coupled Plasma Optical Emission Spectroscopy (ICP-OES)

The metal concentrations within frozen right brain hemispheres and liver samples were processed at the Agricultural Diagnostic Service Center (ADSC) run by the College of Tropical Agriculture and Human Resources (CTAHR), University of Hawaii. Dry ash sample preparations were subjected to acid digest before ICP-OES (.01 ppm detection limit) to measure total brain and liver metal content (Zn^{2+}, Cu^{2+}, Fe^{2+}).

Protein extraction and western blot

Proteins were extracted from frozen hippocampal tissue using Cell Lytic buffer (Sigma) per the manufacturer's instructions, denatured by heating in Laemmli sample buffer, resolved by SDS-PAGE on a 10-20% gradient Tris-HCl Criterion Precast gel (Bio-Rad Laboratories), and electrically transferred to polyvinylidene difluoride (PVDF) membranes. For detection of Zn^{2+} regulating proteins, membranes were incubated in anti-metallothionein-3 (1:500, rabbit polyclonal, Biorbyt), and anti-ZnT1 and anti-ZnT3 (1:1000; 1:5000, rabbit polyclonal, Synaptic Systems). For detection of the Sepp1 protein, membranes were incubated in anti-Sepp1 (1:1000, rabbit monoclonal, Proteintech) and visualized with corresponding fluorescent secondary antibodies (1:10,000; Sigma). Samples were normalized to α-tubulin (1:5000; Novus Biologicals) to control for loading. Membranes were imaged with the Odyssey infrared fluorescence system (LiCor), and densitometry analysis was performed on the Imagestudio software (LiCor).

Metal agarose column purification

To observe Sepp1 binding to biometals, we used mini spin-columns containing agarose

beads conjugated with Zn^{2+}, Ni^{2+}, and Co^{2+} (Agarose Bead Technologies) to isolate metal-binding proteins from wildtype and Sepp1$^{-/-}$ mouse serum. A metal-free agarose column was used as a negative control. Serum samples were diluted 1:100 in PBS and added to the column, shaken for 60 minutes at 4°C, then spun for 60s at 800x g to collect flow-through. Columns were washed with increasing concentrations of imidazole (0, 10, and 20 mM) diluted in PBS, and then bound proteins were eluted with 250 mM imidazole diluted in PBS. Eluted proteins were determined with western blot using an anti-Sepp1 antibody [62].

Live hippocampal slice imaging

To measure release of Zn^{2+} from synaptic vesicles, hippocampal slices were prepared from 3-6 month old Sepp1 KO and wild-type littermate mice as previously described by Bark et al., 2004. Following slice preparation, slices were acclimated to room temperature and superfused with oxygenated (O_2% and 5% CO_2 gas mix) artificial cerebral spinal fluid (ACSF, composition in mM: NaCl, 130; KCl, 3.5; glucose, 10; $NaHCO_3$, 24; NaH_2PO_4, 1.25; $MgSO_4 \cdot 7H_2O$, 1.5; $CaCl_2 \cdot 2H_2O$, 2) for at least 60 minutes. The CA1 stratum radiation region of the slices was imaged with a Zeiss laser microscope using a 10X objective with the pinhole fully open at 1 frame/s at 640x480 resolution. 1.5 μM of a cell-impermeable FluoZin-3 (Molecular Probes) was added in the ACSF of fresh hippocampal slices to detect Zn^{2+} release in response to the administration of a depolarizing (35mM) KCl concentration for 60s, a widely accepted method for depolarizing membrane and inducing neurotransmitter release, then washed with fresh ACSF. In some experiments, a slow onset Zn^{2+} chelator (Ca^{2+}-EDTA) was added to remove contaminating Zn^{2+} in media and to reduce background noise [17]. Mean fluorescence intensity of hippocampal Sepp1$^{-/-}$ slices in the CA1 stratum radiatum region upon addition of KCl were compared to WT to determine if changes in Zn^{2+} release were altered.

Statistical analysis

All statistical analyses were carried out with Graphpad Prism Software with measurements given as means $\pm$ SE. Comparisons between genotypes and gender were performed by student's unpaired t-test and two-way analysis of variance (ANOVA), $p<0.05$ is considered significant.

CHAPTER III

RESULTS

Prediction of Zn^{2+} binding residues within the Sepp1 structure

We used the web-based software Predzinc (http://casio.fos.su.se/server/predzinc/index.php), a web server that predicts zinc-binding proteins and zinc-binding sites from given sequences, to analyze the Sepp1 coding sequences for potential zinc-binding sites. While most algorithms for predicting Zn^{2+} binding require an X-ray crystallography structure for the protein of interest, which is not available for Sepp1, the Predzinc software circumvents this by comparing the protein of interest to zinc-binding proteins with sequence homology. We analyzed human and mouse Sepp1 sequences for potential zinc-binding residues. In addition, we analyzed the sequences after substituting Cys for all Sec residues in case the algorithm did not recognize Sec. We found that a His-residue within the Sepp1 His-rich metal binding domain as well as two other His residues in the C-terminal region are predicted to be Zn^{2+} binding motifs (Figure 4), indicating that Zn^{2+} can only bind to full-length Sepp1.

Confirmed binding of Sepp1 to Zn^{2+} ions in vitro

Because of the predicted Zn^{2+}-binding region of Sepp1, we tested Sepp1's potential to bind Zn^{2+} ions by purifying Sepp1 mouse serum with agarose columns bound to Co^{2+}, Ni^{2+}, or Zn^{2+}. Metal-free agarose columns were used as a negative control. Western blot of sample elution from each column purification shows that Sepp1 binds to Co^{2+}, Ni^{2+}, or Zn^{2+}, but not to the metal-free agarose column (Figure 5). Sepp1 was not detected in the $Sepp1^{-/-}$ serum in each metal binding column. According to the band intensity of Sepp1 in each column, the order of affinity for Sepp1 binding is as follows: $Zn^{2+} > Ni^{2+} > Co^{2+}$. This demonstrates that Sepp1 is capable of binding different biometals, with a higher affinity for Zn^{2+}.

Elevated levels of intracellular Zn^{2+} in $Sepp1^{-/-}$ hippocampus

To explore the effects of Sepp1 on Zn^{2+} ions, we measured intracellular Zn^{2+} levels of $Sepp1^{-/-}$ mice. We initially quantified Zn^{2+} levels in the hippocampus because of its functional importance in learning and memory and its implications in altering synaptic physiology.

By using TSQ labeling, we compared bioreactive Zn^{2+} levels in Sepp1$^{-/-}$ and wildtype mouse hippocampi. Quantitation of TSQ fluorescence revealed significantly higher levels of intracellular Zn^{2+} in the CA1 stratum oriens, stratum radiatum, and CA3 mossy fibers of the Sepp1$^{-/-}$ animals compared to their control (Figure 6). The hilar region showed a similar trend, but the difference was not significant between the two groups. There was also an apparent gender difference in Zn^{2+} levels within the CA3 mossy fiber region with the females having increased cellular Zn^{2+} content, which may contribute to the greater incidence of AD in women than in men (data not shown) [46].

Unstained hippocampal brain sections showed no fluorescence, indicating that differences were not due to autofluorescence. Images taken from the cerebral cortex revealed a lower level of Zn^{2+} content compared to the hippocampus. Hemotoxylin staining of previously TSQ labeled slides showed no morphological differences between Sepp1 wildtype and KO hippocampi. Based on our findings, Sepp1 may be regulating Zn^{2+} levels directly or through one or more Zn^{2+} interacting proteins.

Total brain Zn^{2+} is increased in Sepp1$^{-/-}$ mice

As we observed increased levels of intracellular Zn^{2+} within the hippocampus of Sepp1$^{-/-}$ mice, we then investigated if the total brain Zn^{2+} levels are altered by subjecting whole brain hemispheres via ICP-OES to measure total metal content, specifically Zn^{2+}, Cu^{2+}, and Fe^{2+} (Figure 7).

There was a significant increase in total brain Zn^{2+} levels in Sepp1$^{-/-}$ mice. ICP-OES analysis of total brain Zn^{2+} content coincides with our TSQ labeling data in which there are higher Zn^{2+} levels in the Sepp1$^{-/-}$ hippocampus. Cu^{2+} brain levels were also significantly elevated in Sepp1$^{-/-}$ mice in comparison to wildtype mice. We observed no significant differences in total brain Fe^{2+} within gender or genotype.

To determine if changes in levels of biometals were brain-specific, we also measured metal content in liver, a major site for Sepp1 synthesis. Although there were elevated Zn^{2+} levels in the liver of female mice, no significant changes between genotypes were observed. There were pronounced gender differences in liver Cu^{2+} and Fe^{2+} levels, but not between genotypes. ICP-OES analysis demonstrated that the absence of Sepp1 results in elevated Zn^{2+} and Cu^{2+} levels in whole brain, suggesting a more global regulation of biometals.

Expression levels of Zn^{2+}-interacting proteins

We wanted to determine if Zn^{2+} regulation correlates with expression of certain Zn^{2+} regulating proteins, particularly ZnT1, ZnT3, and MT3, in the hippocampus.

Western blot indicated that ZnT1 and ZnT3 proteins were unchanged in Sepp1$^{-/-}$ animals, but rather MT3 protein expression was increased (Figure 8). This suggests that deletion of the Sepp1 gene does not affect zinc transport, but it upregulates expression of the Zn^{2+} storage protein, MT3. The enhanced expression of MT3 may be a result of a positive feedback mechanism in response to increased Zn^{2+} levels in the Sepp1$^{-/-}$ hippocampus. Due to possible changes in the expression of Zn^{2+}-regulating proteins and intracellular Zn^{2+} levels, we, then, investigated how Sepp1 may affect hippocampal Zn^{2+} release by live Zn^{2+} imaging of hippocampal slices.

Zn^{2+} release is impaired in Sepp1$^{-/-}$ hippocampus in response to neuron depolarization

Most chelatable Zn^{2+} in hippocampal neurons is vesicular at synaptic sites [75]. We investigated if the excess Zn^{2+} content in Sepp1$^{-/-}$ mice can be found in releasable synaptic vesicles. We imaged Zn^{2+} release from hippocampal slices with a selective cell-impermeant fluorescent Zn^{2+} indicator, Fluozin-3, in the extracellular media. After a steady baseline of 60s and upon cell depolarization by the addition of 35mM KCl in the CA1 stratum radiatum region, we reported an increase in fluorescence in both male and female wildtype mice, indicating release of Zn^{2+} into the extracellular space (Figure 9a). In contrast, we observed minimal Zn^{2+} release in the Sepp1$^{-/-}$ hippocampus.

To reduce background fluorescence, we added the Zn^{2+} chelator, Ca^{2+}-EDTA, to the ACSF. A high background fluorescence recording from Zn^{2+} contaminants in the reagents used may be masking any Zn^{2+} release from Sepp1$^{-/-}$ animals. Even in the presence of Ca^{2+}-EDTA, we still observed impaired Zn^{2+} release in the Sepp1$^{-/-}$ animals upon cell depolarization (Figure 9b).

To determine if impaired Zn^{2+} release correlated with a deficiency in brain selenium, we also imaged slices from animals raised on a Se supplemented diet. Se supplementation does not restore Zn^{2+} release in Sepp1$^{-/-}$ animals, as activity levels were similar to that of a Sepp1$^{-/-}$ animal on a regular diet. This delayed response to neuronal stimulation could cause memory impairments and demonstrate the importance of Sepp1 in facilitating synaptic release of Zn^{2+}.

Sepp1 contains a putative metal-binding domain that can potentially bind Zn^{2+} with a high affinity. The absence of Sepp1 increases the levels of hippocampal and total brain Zn^{2+}, alters the expression of Zn^{2+} storage pools possibly to counterbalance the excess Zn^{2+} content, and impairs synaptic Zn^{2+} release from hippocampal neurons. Our results strongly propose that Sepp1 may be participating in the homeostasis of brain Zn^{2+}.

Figure 4. Comparison of human and mouse Sepp1 sequences as well as sequences with all Cys substituted for Sec residues. Predicted Zn^{2+} binding residues as indicated in Predzinc are highlighted in red. There are three common residues in all four sequences that may be true Zn^{2+} binding motifs: 1 His residue in the His-rich zincin sequence (underlined) and 2 Cys residues in the C-terminal domain.

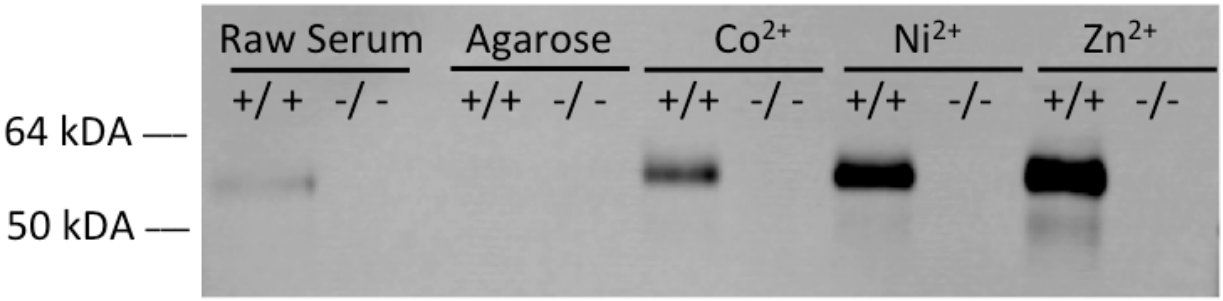

Figure 5. Western blot of metal column eluates after applying mouse serum from WT (+/+) or Sepp1 KO (-/-) mice to mini columns with agarose alone or agarose bound to Co^{2+}, Ni^{2+}, and Zn^{2+}. Untreated $Sepp1^{-/-}$ and WT serum were also added to the blot as a positive control (left lanes). Sepp1 protein detected with anti-Sepp1 antibody (1:1000) had a molecular weight of approximately 55 kDa in the wildtype serum and was not seen in $Sepp1^{-/-}$ serum. Sepp1 was detected in column eluates from wild-type serum applied to all metal columns, but not from columns with agarose alone. Sepp1 protein content was maximally isolated from the Zn^{2+} – agarose column, and decreased in the following order: $Zn^{2+} > Ni^{2+} > Co^{2+}$.

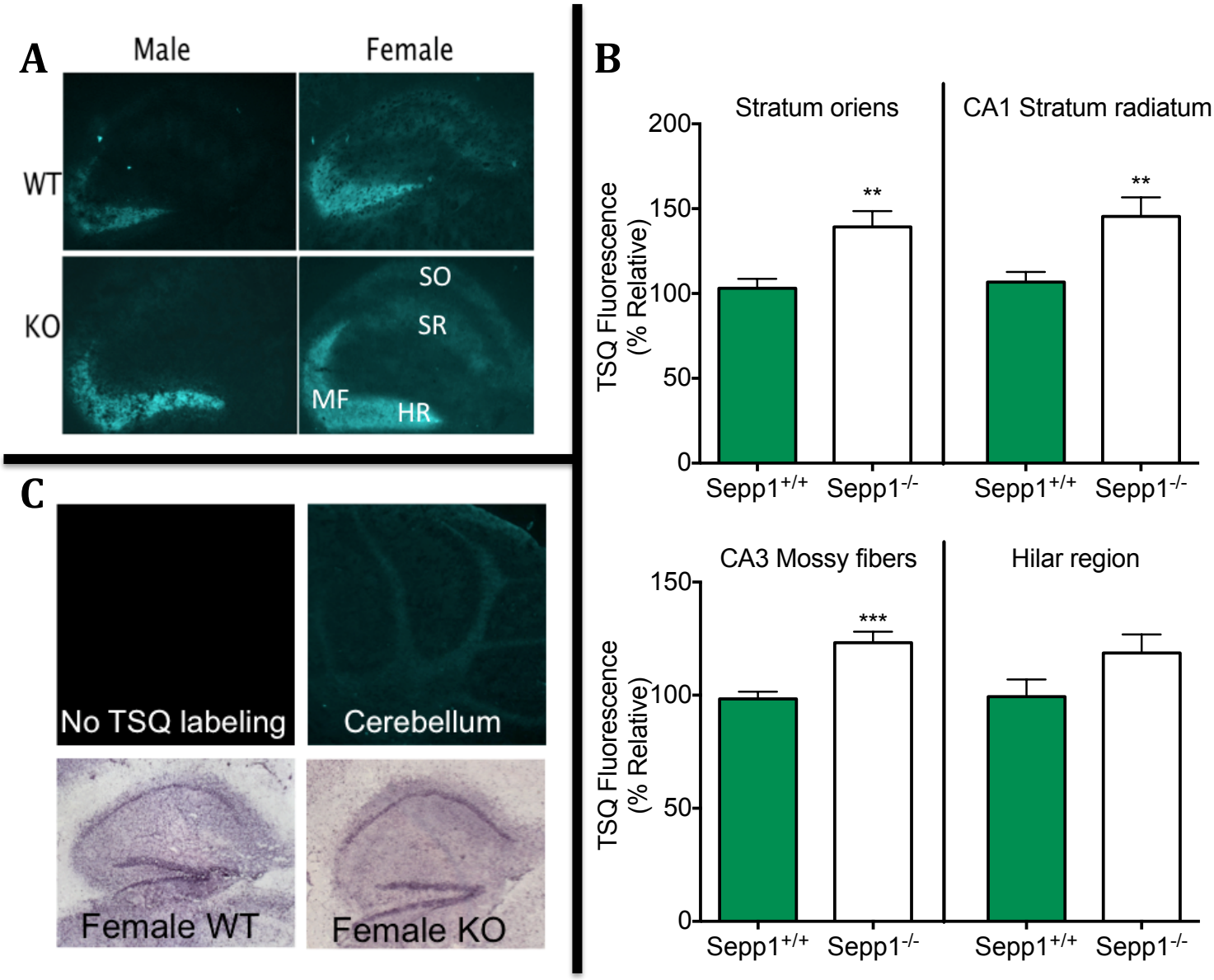

Figure 6. a. Representative images from male and female WT and Sepp1$^{-/-}$ mouse hippocampus, labeled with the fluorescent Zn^{2+} indicator, TSQ. SO: stratum oriens, SR: stratum radiatum, MF: mossy fibers, HR: hilar region. b. Quantitation of TSQ fluorescent label indicates higher Zn^{2+} levels in Sepp1$^{-/-}$ animals in all observed regions except for hilar region. The average values for each region were normalized to wild type males. N = 6 animals/group, 5-10 slices/animal. Statistical analysis is performed by Student's unpaired t-test. **p<0.01, ***p<0.001.

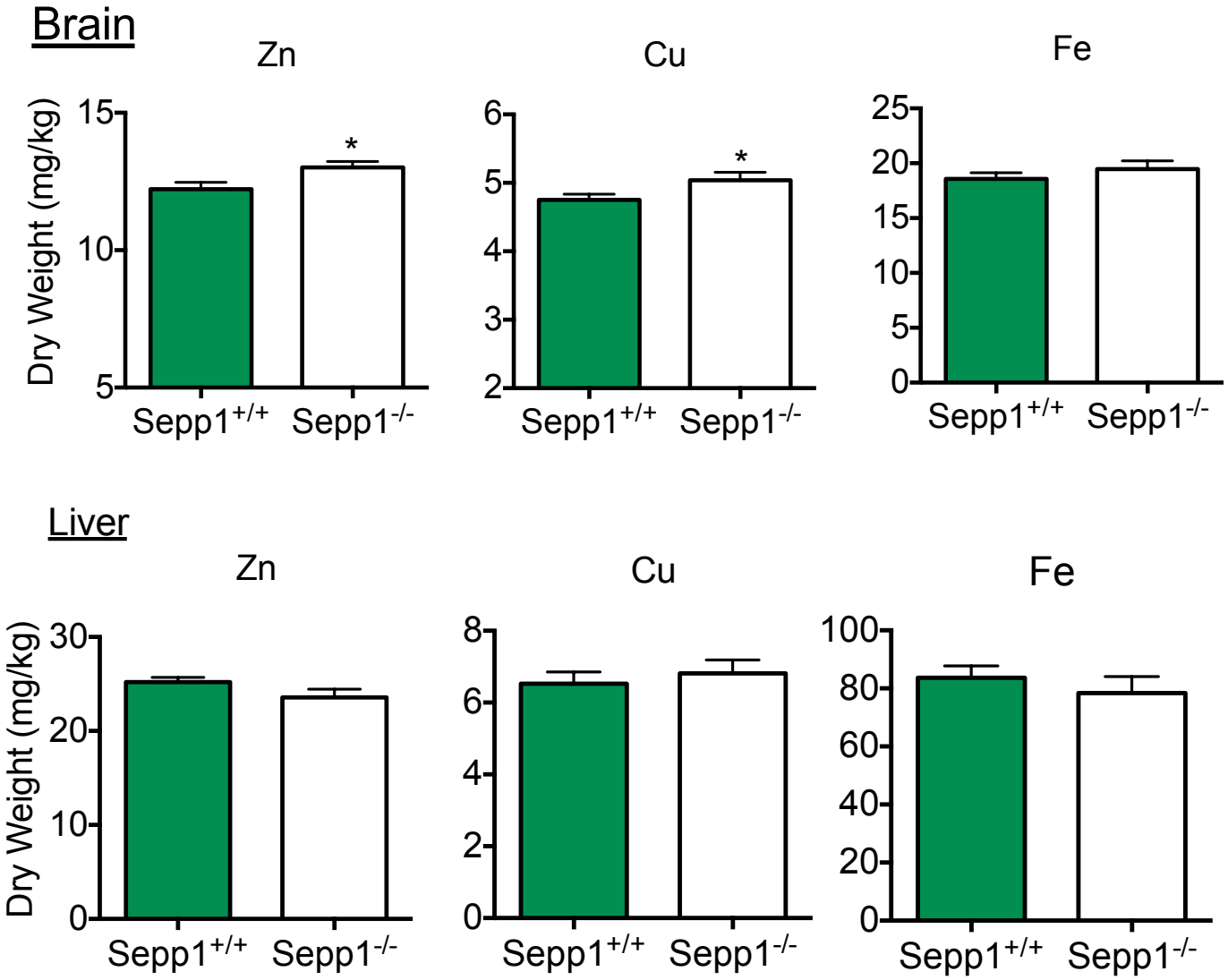

Figure 7. ICP-OES analysis measurements of total metal (Zn^{2+}, Cu^{2+}, Fe^{2+}) levels in whole brain (above) and liver (below) from $Sepp1^{-/-}$ and WT animals. N = 8 animals/group. Statistical analysis is performed by Student's unpaired t-test. *$p<0.05$.

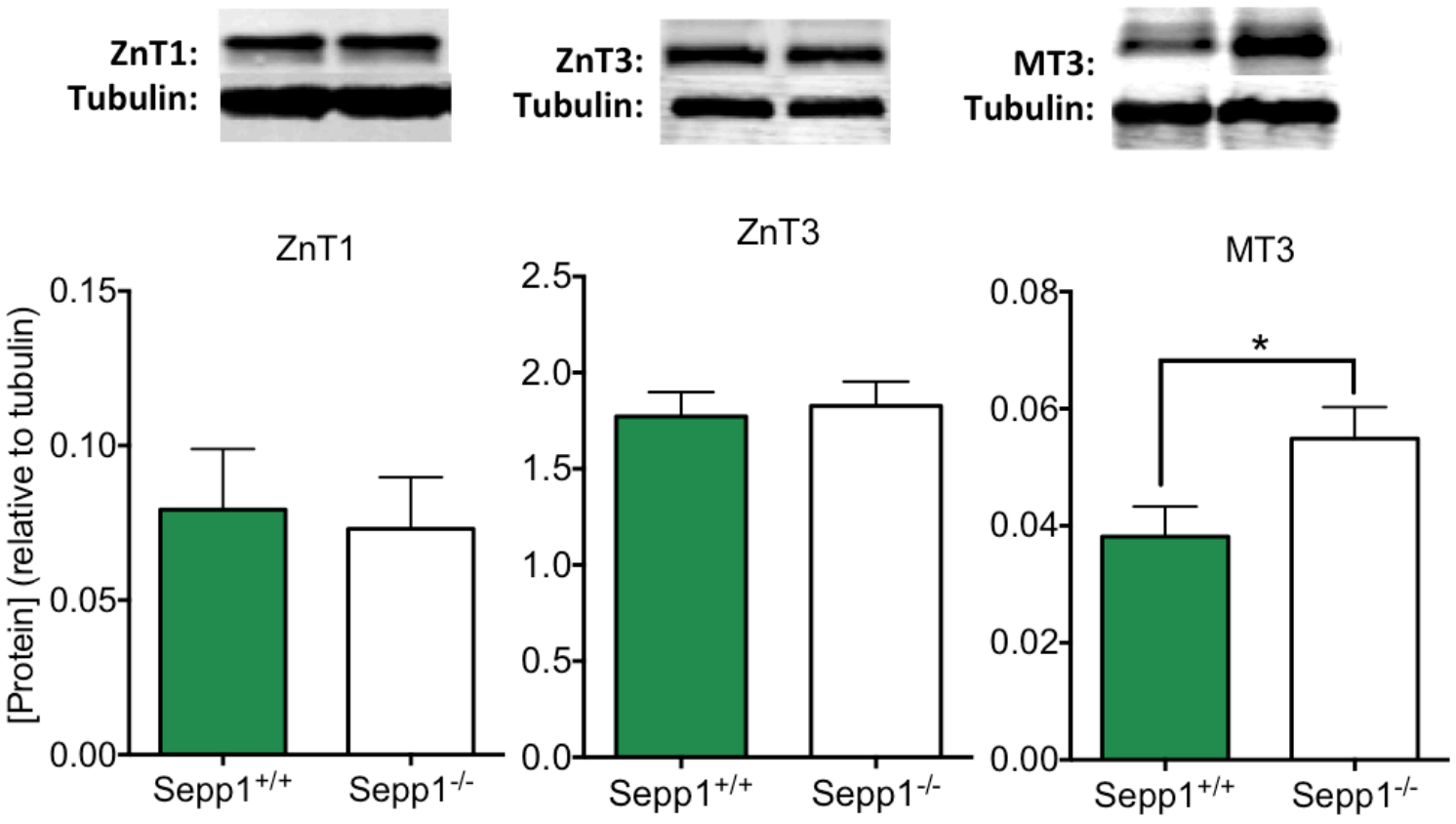

Figure 8. Western blot portraying expression levels of Zn^{2+} transporter proteins, ZnT1 and ZnT3, and Zn^{2+} storage pool, MT3. Protein densities were normalized to alpha tubulin and averaged to male WT values. Protein levels were unchanged in ZnT1 and ZnT3, while increased MT3 expression levels were measured in $Sepp1^{-/-}$ mice. Representative bands are shown above each corresponding bar graph and were found to run at the predicted sizes: ZnT1 (45kDa), ZnT3 (42kDa), and MT3 (40kDa). Statistical analysis is performed by Student's unpaired t-test, *$p<0.05$.

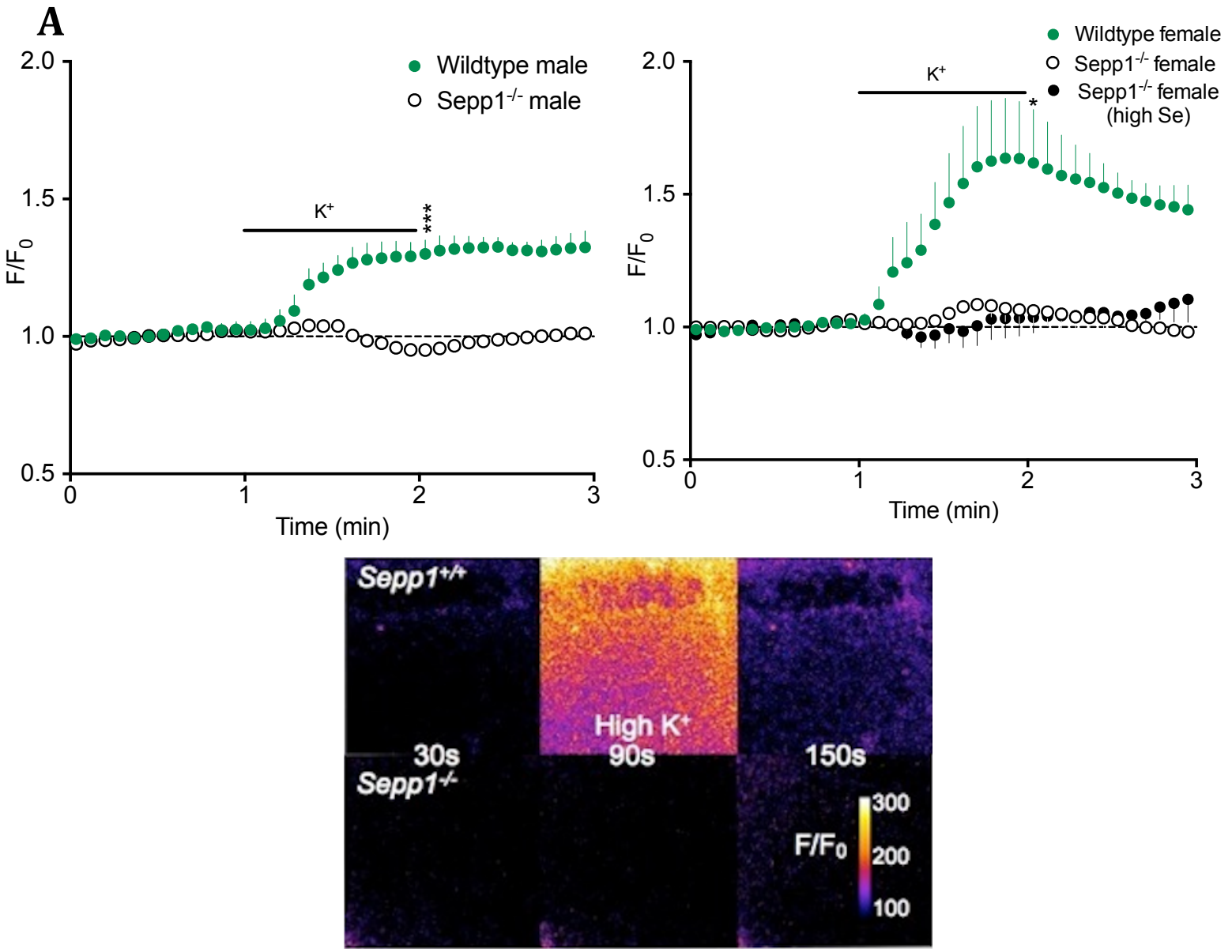

Figure 9a. Zn^{2+} release from hippocampal slices of $Sepp1^{-/-}$ and WT mice visualized with Fluozin-3 following depolarization induced with ACSF containing high (35 mM) KCl solution. Fluorescence in male and female $Sepp1^{-/-}$ hippocampal slices was significantly reduced compared to WT animals. Data plotted as relative fluorescence (F/F_0) over time with measurements averaged every 5s. WT male, n = 3 animals, 6 slices; WT female, n = 3 animals, 4 slices; $Sepp1^{-/-}$ male, n = 3 animals, 6 slices; $Sepp1^{-/-}$ female, n = 4 animals, 6 slices. Below: Representative Fluozin-3 images from WT and $Sepp1^{-/-}$ animals at 30s, 90s, and 150s. Statistical analysis was performed by student's unpaired t-test of values taken from the 2-minute timepoint. *p<0.05, ***p<0.001. Data obtained from $Sepp1^{-/-}$ female slices on a high Se diet were not significant.

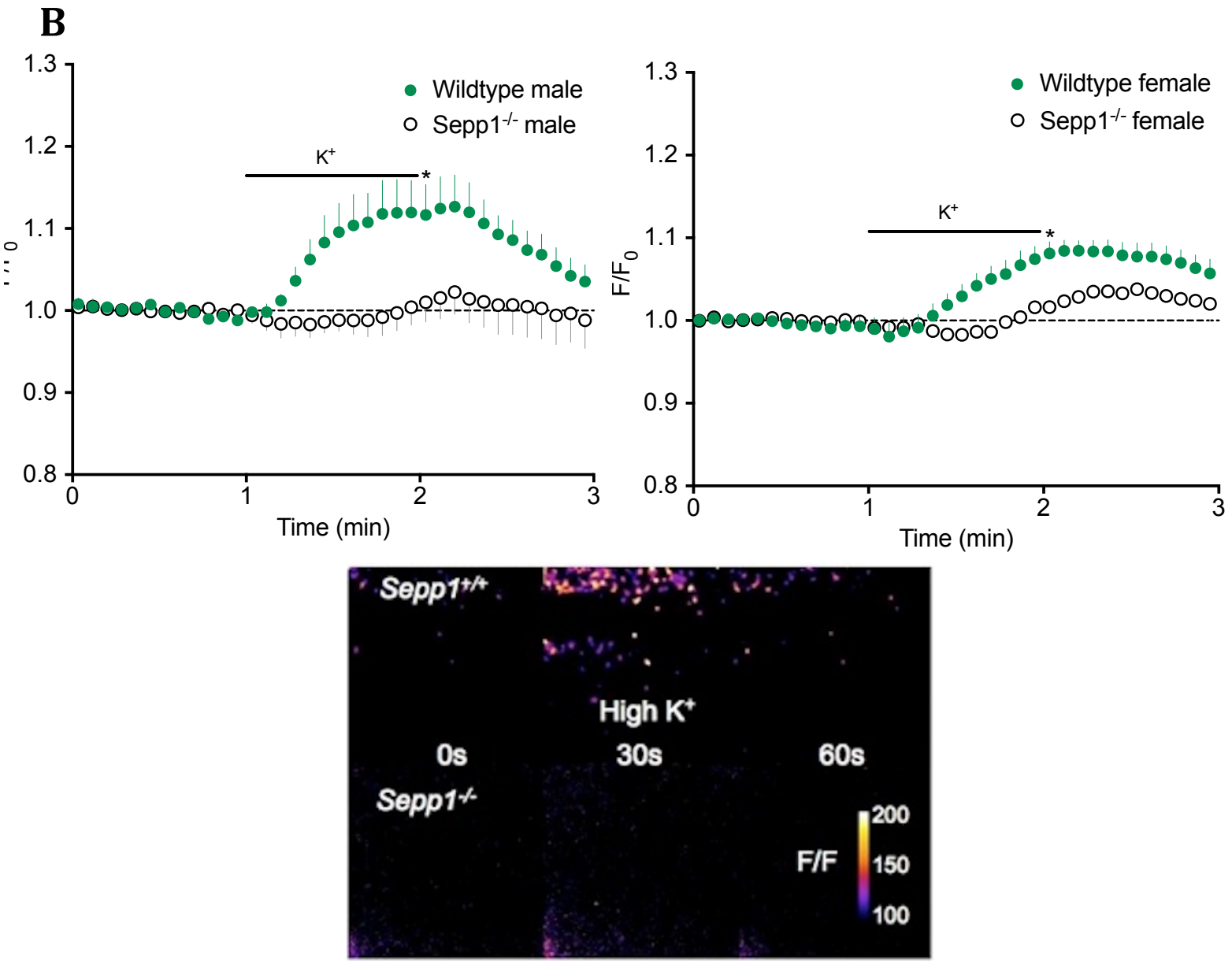

Figure 9b. Zn^{2+} release visualized with Fluozin-3 in ACSF with the addition of Zn^{2+} chelator, Ca^{2+}-EDTA to reduce background fluorescence, following application of ACSF with high (35 mM) KCl. Data plotted as relative fluorescence (F/F_0) over time with measurements averaged every 5s. WT male, n = 3 animals, 4 slices; WT female, n = 4 animals, 7 slices; $Sepp1^{-/-}$ male, n = 3 animals, 5 slices; $Sepp1^{-/-}$ female, n = 3 animals, 5 slices. Fluorescence in male and female $Sepp1^{-/-}$ hippocampal slices was significantly reduced compared to WT animals. Below: Representative Fluozin-3 images from WT and $Sepp1^{-/-}$ animals at 30s, 90s, and 150s. Statistical analysis was performed by Student's unpaired t-test of values taken from the 2-minute timepoint, *$p<0.05$.

CHAPTER IV

DISCUSSION

Our results demonstrate that Sepp1 is capable of binding Zn^{2+} as well as other biometals, Co^{2+}, and Ni^{2+}. Additionally, we have shown that Sepp1$^{-/-}$ mice have increased hippocampal free Zn^{2+} as well as in total brain Zn^{2+} levels. Expression of zinc transporter proteins is not affected by the absence of Sepp1, but there is altered expression of Zn^{2+} storage pools. Finally, we report that synaptic Zn^{2+} release is decreased in the hippocampus of Sepp1$^{-/-}$ mice.

Zn^{2+} and Sepp1 are both associated with Aß plaques in AD. Se is known to have a high affinity for Zn^{2+}, and this property has been applied to various histological methods [69]. However, the physiological function of this interaction and its impact on the human body have not been studied. We demonstrated the ability of Sepp1 to bind different biometals, with apparent affinity for Zn^{2+}, than for Co^{2+}, or Ni^{2+}, awaiting confirmation in metal-Sepp1 binding assays. Since a metal column purification assay is not necessarily reflective of affinity, it would be crucial to perform a binding assay with varying amounts of unbound Zn^{2+} and Sepp1. This supports our finding of a predicted Zn^{2+} motif in the Sepp1 amino acid sequence.

Although we have confirmed Sepp1's ability to bind Zn^{2+} ions *in vitro*, it is not clear as to whether Zn^{2+} is interacting with the predicted Zn^{2+}-binding residues or the Sec residues, which may have good Zn^{2+} binding ability as well, or both. This may give Sepp1 some special binding properties compared to other Zn^{2+} binding proteins. Due to the individual roles of Sepp1 and Zn^{2+} in neurodegenerative diseases such as AD and the potential presence of a Zn^{2+} binding region within the Sepp1 structure, we investigated whether Sepp1 may modulate Zn^{2+} homeostasis in the brain.

In the absence of Sepp1, we observed a paradoxical impairment of Zn^{2+} release despite an overall increase in intracellular Zn^{2+}. Sepp1 could be interacting with ZnT3 to aid in the packaging and loading of Zn^{2+} into the synaptic vesicles [32, 50], with Sepp1 deletion resulting in reduced Zn^{2+} in the synaptic vesicles, and/or assist ZntT1 in exporting vesicles out of the presynaptic terminals [58]. Sepp1 may also be directly controlling synaptic Zn^{2+} release or indirectly via ApoER2 signaling. An explanation for our findings could be that the

excess Zn^{2+} measured through TSQ staining and ICP-OES is thus non-vesicular. Therefore, Sepp1 may be involved in three distinct roles: 1) synaptic release of Zn^{2+} vesicles, 2) packaging and loading of Zn^{2+} into vesicles via Zn^{2+} transporter proteins and 3) modulation of overall Zn^{2+} homeostasis as a transient chelator of excess non-vesicular Zn^{2+} with its predicted zinc-binding site.

The aberrant Zn^{2+} response to depolarization in Sepp1 null mutant preparations suggests a function of Sepp1 in synaptic transmission and synaptic plasticity. The lack of Zn^{2+} release into the synaptic cleft may hinder its ability to modulate overall excitability of the brain by binding to essential postsynaptic receptors, such as NMDA, to regulate LTP, thus contributing to cognitive decline. This observation may correlate with known behavioral and neurological traits of $Sepp1^{-/-}$ mice such as deficiencies in synaptic hippocampal function, disrupted spatial learning, and a severe LTP deficit even when fed on a high Se diet [60]. Our live Zn^{2+} imaging shows that synaptic Zn^{2+} release is not restored in mice raised on a supplemented Se diet.

The increased levels of certain Zn^{2+}-storage proteins such as MT3 might accommodate for the enhanced Zn^{2+} content. The absence of Sepp1 could induce oxidative stress in the brain and lead to Zn^{2+} release from MT3. Since MT3 provides short term Zn^{2+} storage, upregulation of Zn^{2+} storage pools may be crucial. Overexpression of MT3 in $Sepp1^{-/-}$ mice may affect the subcellular distribution of Zn^{2+} by limiting the amount of free Zn^{2+} available for loading into the synaptic vesicles.

Although ZnT3 levels are unchanged, it is possible that ZnT3 proteins are not properly bound to the synaptic vesicles, thus impairing its function to package and load vesicular Zn^{2+} due to the reduction of AP3δ expression in $Sepp1^{-/-}$ mice. AP3δ is responsible for post-translational stability of ZnT3 and insertion of ZnT3 into the vesicles [75]. ZnT3 expression without AP3δ may explain the lack of function in Zn^{2+} transport in places where ZnT3 protein is detected [45].

Zn^{2+} metabolism is altered in AD resulting in abnormally enriched Zn^{2+} environments within the AD brain [30]. Zinc-binding sites on the Aß peptide result in Zn^{2+} mediated aggregation of Aß and amyloid plaque formation. High dietary Zn^{2+} levels may contribute to the pathophysiology of AD by enhancing Aβ generation and aggregation through modifying expression of APP levels and APP cleavage enzymes *in vivo* and *in vitro*. This may result in

cognition dysfunction [18]. Furthermore, due to Sepp1's neuroprotective role against Aß toxicity and Zn^{2+}'s function in protecting the cell against oxidative damage, both entities could be working together to reduce the levels of Aβ stress observed in AD pathology, however more studies need to be done to further elucidate their contribution to alleviating oxidative stress.

There have also been neurological manifestations of copper deficiency in response to high Zn^{2+} intake [53], which contradicts our finding of increased total Cu^{2+} levels in whole brain samples. Low levels of extracellular Cu^{2+}, similarly to Zn^{2+}, can contribute to Aß by altering its clearance and production in the brain [64]; however Cu^{2+}'s role in synaptic transmission is not well understood. It is possible that Sepp1's metal-binding property also participates in Cu^{2+} metabolism, which needs to be investigated further.

Since upregulation of Sepp1 is age-dependent, age may also be a factor in the homeostasis of Zn^{2+}. Zn^{2+} deficiency leads to loss of immunological responses due to the impairment of neuroendocrine function and increased apoptosis [18]. Our results, however, show an excess of Zn^{2+} when Sepp1 is not expressed, which may indicate that although Sepp1 is age-dependent, it might be involved in a pathway distinct from Zn^{2+}'s role in aging.

The data presented here indicate that Sepp1 may play a crucial role in the maintenance of Zn^{2+} homeostasis in the hippocampus and for proper brain function. The Sepp1 gene can affect Zn^{2+} metabolism and synaptic release from neuronal synapses with implications in synaptic physiology and in the prevention of Aß into amyloid plaques. The potential role of Sepp1 in brain homeostasis of Zn^{2+} may be important in developing treatments for AD, especially as Sepp1 levels are easily controlled by dietary Se intake.

Future directions

To further characterize the biological significance of the interaction between Sepp1 and Zn^{2+} in the brain, it would be critical to carry out future studies. Further studying how MT3 is regulated in the absence of Sepp1 (transcriptional or translational) would be beneficial to understanding the potential positive feedback mechanism occurring in the presence of excess Zn^{2+}. To determine whether ZnT3 is not properly inserted into the synaptic vesicle membrane due to changes in AP3δ expression in the $Sepp1^{-/-}$ mouse model, we could isolate the presynaptic vesicles and measure protein levels of ZnT3 and AP3δ. In addition, a ZnT3 and Sepp1 double-knockout mouse model could demonstrate if the excess Zn^{2+} observed in the $Sepp1^{-/-}$ brain is eliminated and if synaptic Zn^{2+} release is affected. Finally, by performing electrophysiology with advanced synaptic Zn^{2+} imaging, we could have an accurate description of the dynamics of activity dependent Zn^{2+} release.

REFERENCES

1. Adlard, P.A. et al. (2008) Rapid restoration of cognition in Alzheimer's transgenic mice with 8-hydroxy quinoline analogs is associated with decreased interstitial Abeta. *Neuron*, **59**, 43-55.

2. Adlard, P.A. & Bush, A.I. (2006) Metals and Alzheimer's disease. *J Alzheimers Dis*, **10**, 145-163.

3. Areosa, S.A., Sherriff, F. & McShane, R. (2005) Memantine for dementia. *Cochrane Database Syst Rev*, CD003154.

4. Ballatore, C., Lee, V.M. & Trojanowski, J.Q. (2007) Tau-mediated neurodegeneration in Alzheimer's disease and related disorders. *Nat Rev Neurosci*, **8**, 663-672.

5. Bartus, R.T. (2000) On neurodegenerative diseases, models, and treatment strategies: lessons learned and lessons forgotten a generation following the cholinergic hypothesis. *Experimental neurology*, **163**, 495-529.

6. Beckett, G.J. & Arthur, J.R. (2005) Selenium and endocrine systems. *J Endocrinol*, **184**, 455-465.

7. Bellinger, F.P. et al. (2009) Regulation and function of selenoproteins in human disease. *Biochem J*, **422**, 11-22.

8. Bellinger, F.P. et al. (2008) Association of selenoprotein p with Alzheimer's pathology in human cortex. *J Alzheimers Dis*, **15**, 465-472.

9. Berry, M.J. et al. (1993) Functional characterization of the eukaryotic SECIS elements which direct selenocysteine insertion at UGA codons. *EMBO J*, **12**, 3315-3322.

10. Bothwell, D.N., Mair, E.A. & Cable, B.B. (2003) Chronic ingestion of a zinc-based penny. *Pediatrics*, **111**, 689-691.

11. Burk, R.F. & Hill, K.E. (2009) Selenoprotein P-expression, functions, and roles in mammals. *Biochim Biophys Acta*, **1790**, 1441-1447.

12. Burk, R.F. et al. (2007) Deletion of apolipoprotein E receptor-2 in mice lowers brain selenium and causes severe neurological dysfunction and death when a low-selenium diet is fed. *J Neurosci*, **27**, 6207-6211.

13. Burk, R.F. & Hill, K.E. (2005) Selenoprotein P: an extracellular protein with unique physical characteristics and a role in selenium homeostasis. *Annu Rev Nutr*, **25**, 215-235.

14. Bush, A.I. & Tanzi, R.E. (2008) Therapeutics for Alzheimer's disease based on the metal hypothesis. *Neurotherapeutics*, **5**, 421-432.

15. Butterfield, D.A., Perluigi, M. & Sultana, R. (2006) Oxidative stress in Alzheimer's disease brain: new insights from redox proteomics. *European journal of pharmacology*, **545**, 39-50.

16. Carlo, A.S. (2013) Sortilin, a novel APOE receptor implicated in Alzheimer disease. *Prion*, **7(5)**,

17. Carter, R.E. et al. (2010) Spreading depression and related events are significant sources of neuronal Zn2+ release and accumulation. *Journal of Cerebral Blood Flow & Metabolism*, **31**, 1073-1084.

18. Chasapis, C.T. et al. (2012) Zinc and human health: an update. *Arch Toxicol*, **86**, 521-534.

19. Cherny, R.A. et al. (2001) Treatment with a copper-zinc chelator markedly and rapidly inhibits beta-amyloid accumulation in Alzheimer's disease transgenic mice. *Neuron*, **30**, 665-676.

20. Chorin, E. et al. (2011) Upregulation of KCC2 activity by zinc-mediated neurotransmission via the mZnR/GPR39 receptor. *J Neurosci*, **31**, 12916-12926.

21. Clare, R. et al. (2010) Synapse loss in dementias. *J Neurosci Res*, **88**, 2083-2090.

22. Clark, C.M. et al. (2011) Use of florbetapir-PET for imaging beta-amyloid pathology. *JAMA*, **305**, 275-283.

23. Cole, T.B., Martyanova, A. & Palmiter, R.D. (2001) Removing zinc from synaptic vesicles does not impair spatial learning, memory, or sensorimotor functions in the mouse. *Brain Res*, **891**, 253-265.

24. Corcoran, N.M. et al. (2010) Sodium selenate specifically activates PP2A phosphatase, dephosphorylates tau and reverses memory deficits in an Alzheimer's disease model. *J Clin Neurosci*, **17**, 1025-1033.

25. Corder, E.H. et al. (1993) Gene dose of apolipoprotein E type 4 allele and the risk of Alzheimer's disease in late onset families. *Science*, **261**, 921-923.

26. Coyle, P. et al. (2002) Metallothionein: the multipurpose protein. *Cell Mol Life Sci*, **59**, 627-647.

27. Doraiswamy, P.M. & Xiong, G.L. (2006) Pharmacological strategies for the prevention of Alzheimer's disease. *Expert Opin Pharmacother*, **7**, 1-10.

28. Du, X. et al. (2013) Selenoprotein P and selenoprotein M block Zn2+ -mediated Abeta42 aggregation and toxicity. *Metallomics*, **5**, 861-870.

29. Farlow, M.R., Graham, S.M. & Alva, G. (2008) Memantine for the treatment of Alzheimer's disease: tolerability and safety data from clinical trials. *Drug Saf*, **31**, 577-585.

30. Faller, P. (2009) Copper and zinc binding to amyloid-beta: coordination, dynamics, aggregation, reactivity and metal-ion transfer. *Chembiochem*, **10**, 2837-2845.

31. Franson, J.C. et al. (2007) Effects of dietary selenium on tissue concentrations, pathology, oxidative stress, and immune function in common eiders (Somateria mollissima). *J Toxicol Environ Health A*, **70**, 861-874.

32. Frederickson, C.J., Koh, J.Y. & Bush, A.I. (2005) The neurobiology of zinc in health and disease. *Nat Rev Neurosci*, **6**, 449-462.

33. Frederickson, C.J. et al. (1987) A quinoline fluorescence method for visualizing and assaying the histochemically reactive zinc (bouton zinc) in the brain. *Journal of neuroscience methods*, **20**, 91-103.

34. Gaither, L.A. & Eide, D.J. (2000) Functional expression of the human hZIP2 zinc transporter. *J Biol Chem*, **275**, 5560-5564.

35. Golde, T.E. et al. (1992) Processing of the amyloid protein precursor to potentially amyloidogenic derivatives. *Science*, **255**, 728-730.

36. Gomis-Ruth, F.X. (2003) Structural aspects of the metzincin clan of metalloendopeptidases. *Mol Biotechnol*, **24**, 157-202.

37. Grundke-Iqbal, I. et al. (1986) Abnormal phosphorylation of the microtubule-associated protein tau (tau) in Alzheimer cytoskeletal pathology. *Proc Natl Acad Sci U S A*, **83**, 4913-4917.

38. Hardy, J. & Selkoe, D.J. (2002) The amyloid hypothesis of Alzheimer's disease: progress and problems on the road to therapeutics. *Science*, **297**, 353-356.

39. Holben, D.H. & Smith, A.M. (1999) The diverse role of selenium within selenoproteins: a review. *J Am Diet Assoc*, **99**, 836-843.

40. Holtzman, D.M., John, C.M. & Goate, A. (2011) Alzheimer's disease: the challenge of the second century. *Science translational medicine*, **3**, 77sr1.

41. Huang, L. & Gitschier, J. (1997) A novel gene involved in zinc transport is deficient in the lethal milk mouse. *Nat Genet*, **17**, 292-297.

42. Huse, J.T. & Doms, R.W. (2001) Neurotoxic traffic: uncovering the mechanics of amyloid production in Alzheimer's disease. *Traffic*, **2**, 75-81.

43. Izumi, Y., Tokuda, K. & Zorumski, C.F. (2008) Long-term potentiation inhibition by low-level N-methyl-D-aspartate receptor activation involves calcineurin, nitric oxide, and p38 mitogen-activated protein kinase. *Hippocampus*, **18**, 258-265.

44. Kang, J. et al. (1987) The precursor of Alzheimer's disease amyloid A4 protein resembles a cell-surface receptor. *Nature*, **325**, 733-736.

45. Kantheti, P. et al. (1998) Mutation in AP-3 delta in the mocha mouse links endosomal transport to storage deficiency in platelets, melanosomes, and synaptic vesicles. *Neuron*, **21**, 111-122.

46. Katzman, R. (1989). Alzheimer's disease is a degenerative disorder. *Neurobiol Aging* **10**, 581-582; discussion 588-590.

47. Kim, J., Basak, J.M. & Holtzman, D.M. (2009) The role of apolipoprotein E in Alzheimer's disease. *Neuron*, **63**, 287-303.

48. King, J.C., Shames, D.M. & Woodhouse, L.R. (2000) Zinc homeostasis in humans. *J Nutr*, **130**, 1360S-1366S.

49. Lee, J.Y. et al. (2012) Alteration of the cerebral zinc pool in a mouse model of Alzheimer disease. *J Neuropathol Exp Neurol*, **71**, 211-222.

50. Lovell, M.A. et al. (2009) Organoselenium (Sel-Plex diet) decreases amyloid burden and RNA and DNA oxidative damage in APP/PS1 mice. *Free Radic Biol Med*, **46**, 1527-1533.

51. Lu, J. & Holmgren, A. (2009) Selenoproteins. *J Biol Chem*, **284**, 723-727.

52. Maret, W. & Sandstead, H.H. (2006) Zinc requirements and the risks and benefits of zinc supplementation. *J Trace Elem Med Biol*, **20**, 3-18.

53. McMahon, R.J. & Cousins, R.J. (1998) Regulation of the zinc transporter ZnT-1 by dietary zinc. *Proc Natl Acad Sci U S A*, **95**, 4841-4846.

54. Meeusen, J.W. et al. (2011) TSQ (6-methoxy-8-p-toluenesulfonamido-quinoline), a common fluorescent sensor for cellular zinc, images zinc proteins. *Inorg Chem*, **50**, 7563-7573.

55. Novoselov, S.V. et al. (2007) Selenoprotein H is a nucleolar thioredoxin-like protein

with a unique expression pattern. *J Biol Chem*, **282**, 11960-11968.

56. Palmiter, R.D. et al. (1996) ZnT-3, a putative transporter of zinc into synaptic vesicles. *Proc Natl Acad Sci U S A*, **93**, 14934-14939.

57. Palmiter, R.D. & Findley, S.D. (1995) Cloning and functional characterization of a mammalian zinc transporter that confers resistance to zinc. *EMBO J*, **14**, 639-649.

58. Perrin, R.J., Fagan, A.M. & Holtzman, D.M. (2009) Multimodal techniques for diagnosis and prognosis of Alzheimer's disease. *Nature*, **461**, 916-922.

59. Peters, M.M. et al. (2006) Altered hippocampus synaptic function in selenoprotein P deficient mice. *Mol Neurodegener*, **1**, 12.

60. Reinikainen, K.J., Soininen, H. & Riekkinen, P.J. (1990) Neurotransmitter changes in Alzheimer's disease: implications to diagnostics and therapy. *Journal of neuroscience research*, **27**, 576-586.

61. Seale, L.A. et al. (2012) Disruption of the selenocysteine lyase-mediated selenium recycling pathway leads to metabolic syndrome in mice. *Mol Cell Biol*, **32**, 4141-4154.

62. Selenius, M. et al. (2010) Selenium and the selenoprotein thioredoxin reductase in the prevention, treatment and diagnostics of cancer. *Antioxid Redox Signal*, **12**, 867-880.

63. Sensi, S.L. et al. (2009) Zinc in the physiology and pathology of the CNS. *Nature reviews neuroscience*, **10**, 780-791.

64. Singh, S.K. et al. (2013) Neuroprotective Role of a Novel Copper Chelator against Abeta 42 Induced Neurotoxicity. *Int J Alzheimers Dis*, **2013**, 567128.

65. Small-Howard, A.L. & Berry, M.J. (2005) Unique features of selenocysteine incorporation function within the context of general eukaryotic translational processes. *Biochem Soc Trans*, **33**, 1493-1497.

66. Squires, J.E. & Berry, M.J. (2008) Eukaryotic selenoprotein synthesis: mechanistic insight incorporating new factors and new functions for old factors. *IUBMB Life*, **60**, 232-235.

67. Stefanidou, M. et al. (2006) Zinc: a multipurpose trace element. *Arch Toxicol*, **80**, 1-9.

68. Steinbrenner, H. et al. (2006) Involvement of selenoprotein P in protection of human astrocytes from oxidative damage. *Free Radic Biol Med*, **40**, 1513-1523.

69. Stoltenberg, M. et al. (2005) Immersion autometallographic tracing of zinc ions in Alzheimer beta-amyloid plaques. *Histochem Cell Biol*, **123**, 605-611.

70. Suh, S.W. et al. (2005) Adrenalectomy-induced ZnT3 downregulation in mouse hippocampus is followed by vesicular zinc depletion. *Neurosci Lett*, **377**, 164-169.

71. Takeda, A. et al. (2009) Unique response of zinc in the hippocampus to behavioral stress and attenuation of subsequent mossy fiber long-term potentiation. *Neurotoxicology*, **30**, 712-717.

72. Takemoto, A.S., Berry, M.J. & Bellinger, F.P. (2010) Role of selenoprotein P in Alzheimer's disease. *Ethn Dis*, **20**, S1-92-5.

73. Thies, W. & Bleiler, L. (2013) 2013 Alzheimer's disease facts and figures Alzheimer's Association. *ALZHEIMERS & DEMENTIA*, **9**, 208-245.

74. Tung, Y.T. et al. (2008) Sodium selenite inhibits gamma-secretase activity through activation of ERK. *Neurosci Lett*, **440**, 38-43.

75. Valente, T. & Auladell, C. (2002) Developmental expression of ZnT3 in mouse brain: correlation between the vesicular zinc transporter protein and chelatable vesicular zinc (CVZ) cells. Glial and neuronal CVZ cells interact. *Mol Cell Neurosci*, **21**, 189-204.

76. Wang, H. & Zhuo, M. (2012) Group I metabotropic glutamate receptor-mediated gene transcription and implications for synaptic plasticity and diseases. *Front Pharmacol*, **3**, 189.

77. Xia, L. et al. (2003) The mammalian cytosolic selenoenzyme thioredoxin reductase reduces ubiquinone. A novel mechanism for defense against oxidative stress. *J Biol Chem*, **278**, 2141-2146.

78. Xiong, S. et al. (2007) Seleno-L-methionine protects against beta-amyloid and iron/hydrogen peroxide-mediated neuron death. *Antioxid Redox Signal*, **9**, 457-467.

79. Xuan, Y. et al. (2012) Zinc finger antiviral protein inhibits murine gammaherpesvirus 68 M2 expression and regulates viral latency in cultured cells. *J Virol*, **86**, 12431-12434.

80. Zhang, Y.H. et al. (2013) Efficacy and toxicity of clioquinol treatment and A-beta42 inoculation in the APP/PSI mouse model of Alzheimer's disease. *Curr Alzheimer Res*, **10**, 494-506.